Molecular Pharmacology Fast Forward. Published on August 23, 2012 as doi:10.1124/mol.112.080036

Generation and characterization of novel Cytochrome P450 Cyp2c gene cluster knockout and CYP2C9 humanized mouse lines

Nico Scheer, Yury Kapelyukh, Lynsey Chatham, Anja Rode, Sandra Buechel and C Roland Wolf

TaconicArtemis, Neurather Ring 1, Koeln 51063, Germany (NS, AR, SB).

CXR Biosciences Limited, 2 James Lindsay Place, Dundee, DD1 5JJ, United Kingdom (YK, CRW).

Cancer Research UK Molecular Pharmacology Unit, Medical Research Institute, Ninewells Hospital and Medical School, University of Dundee, Dundee DD1 9SY, United Kingdom (CRW).

Division of Cancer Research, Medical Research Institute, Level 9, Jacqui Wood Cancer Centre, University of Dundee, James Arrott Drive, Ninewells Hospital & Medical School, Dundee, DD1 9SY, United Kingdom (LC).

Molecular Pharmacology Fast Forward. Published on August 23, 2012 as DOI: 10.1124/mol.112.080036
This article has not been copyedited and formatted. The final version may differ from this version.

Running title: Cyp2c knockout and CYP2C9 humanized mice

Address correspondence to:

Nico Scheer, PhD, TaconicArtemis, Neurather Ring 1, 51063 Koeln, Germany.

Tel.: +49 221 9645343; Fax: +49 221 9645321; Email: nico.scheer@taconicartemis.com

Number of text pages: 23

Number of Tables: 0

Number of Figures: 6

Number of references: 34

Number of words in Abstract: 244

Number of words in Introduction: 749

Number of words in Discussion: 1009

Nonstandard abbreviations used:

BAC, bacterial artificial chromosome; CYP/Cyp, Cytochrome P450; Cyp2c KO, Cyp2c knockout mice; ES cells, embryonic stem cells; hCYP2C9, CYP2C9 humanized mice; HLM, human liver microsomes

Molecular Pharmacology Fast Forward. Published on August 23, 2012 as DOI: 10.1124/mol.112.080036
This article has not been copyedited and formatted. The final version may differ from this version.

Abstract

Compared to rodents and many other animal species the human cytochrome P450 *Cyp2c* gene cluster varies significantly in the multiplicity of functional genes and in the substrate specificity of its enzymes. As a consequence, the use of wild type animal models to predict the role of human CYP2C enzymes to drug metabolism and drug-drug interactions is limited. Within the human *CYP2C* cluster CYP2C9 is of particular importance, because it is one of the most abundant P450 enzymes in human liver and it is involved in the metabolism of a wide variety of important drugs and environmental chemicals. In order to investigate the in vivo functions of cytochrome P450 *Cyp2c* genes and to establish a model for studying the functions of CYP2C9 in vivo, we have generated a mouse model with a deletion of the murine *Cyp2c* gene cluster and a corresponding humanized model expressing CYP2C9 specifically in the liver. Despite the high number of functional genes in the mouse *Cyp2c* cluster and the reported roles of some of these proteins in different biological processes, mice deleted for *Cyp2c* genes were viable and fertile but showed certain phenotypic alterations in the liver. The expression of CYP2C9 in the liver also resulted in viable animals active in the metabolism and disposition of a number of CYP2C9 substrates. These mouse lines provide a powerful tool for studying the role of *Cyp2c* genes, and of CYP2C9 in particular, in drug disposition and as a factor in drug-drug interaction.

Molecular Pharmacology Fast Forward. Published on August 23, 2012 as DOI: 10.1124/mol.112.080036
This article has not been copyedited and formatted. The final version may differ from this version.

Introduction

The heme-containing cytochrome P450 (CYPs) enzymes play a central role in the oxidative metabolism of a vast range of small molecule substrates, such as endogenous compounds, environmental chemicals and drugs. Though fifty seven P450 enzymes have been described in humans (Nelson et al., 2004), only a small number account for the majority of P450-mediated metabolism of clinically used drugs. In this regard it has been estimated that ~95% of drug metabolism is mediated by either CYP3A4/5, CYP2D6, CYP2C9/2C19 or CYP1A1/1A2 (Guengerich, 2008). In order to overcome the differences which exist in the substrate specificity, regulation of expression and multiplicity of CYPs between species significant efforts have been made in recent years to humanize mice for some of these key metabolic enzymes, the aim being to provide animal models that better predict human pathways of drug metabolism. In this regard, humanized mouse models for CYP3A4 (Cheung et al., 2006; Hasegawa et al., 2011; van Herwaarden et al., 2007), CYP2D6 (Corchero et al., 2001; Scheer et al., 2012), CYP2C19 (Lofgren et al., 2008) and CYP1A1/1A2 (Cheung et al., 2005; Dragin et al., 2007; Jiang et al., 2005) have been created using a variety of different approaches, either with or without deletion of the corresponding mouse genes. In addition, fertile and viable knockout models of the mouse *Cyp3a* (Hasegawa et al., 2011; van Herwaarden et al., 2007), *Cyp2d* (Scheer et al., 2012) and *Cyp1a* (Dragin et al., 2007) gene clusters have been described, which are associated with only minor overt phenotypic changes compared to WT controls.

The mouse and the human *CYP2C* cluster differ significantly in their genomic organization, with 15 functional genes described in mice compared to only four genes in human (Nelson et al., 2004). Because of these differences in multiplicity, but also in sequence variation, it is not possible to define orthologous genes between both species. Fourteen of the functional genes within the mouse *Cyp2c* cluster are located in close proximity within approximately 1.2 Mb

Molecular Pharmacology Fast Forward. Published on August 23, 2012 as DOI: 10.1124/mol.112.080036
This article has not been copyedited and formatted. The final version may differ from this version.

of mouse chromosome 19, while *Cyp2c44*, albeit on the same chromosome, is separated from the other genes by approximately 4 Mb (Nelson et al., 2004). The four functional genes within the human *CYP2C* cluster are *CYP2C8*, *CYP2C9*, *CYP2C18* and *CYP2C19*. Together they account for approximately 25% of all P450-mediated hepatic drug metabolism (Guengerich, 2008; Williams et al., 2004). Amongst the human CYP2C enzymes CYP2C9 is of key importance, because, apart from CYP3A4, it is the largest contributor to the total human liver microsomal P450 content. CYP2C9 is involved in the disposition of some major classes of therapeutic drugs, including anticoagulants and non-steroidal anti-inflammatory agents, such as warfarin or diclofenac, respectively. It has been estimated to be responsible for the metabolic clearance of up to 15% of all drugs that undergo Phase I metabolism and has been associated with a number of drug-drug interactions. CYP2C9 is also polymorphic in the human population, with a number of null or low activity alleles and such polymorphisms are directly linked to the adverse effects of, for example, warfarin (Rettie and Jones, 2005; Stubbins et al., 1996).

Despite their important role in drug metabolism and the significant species differences in *Cyp2c* genes there are only a few published reports on humanized mouse models. A mouse humanized for CYP2C18/19 which expressed catalytically active CYP2C19 in the liver and intestine has recently been reported (Lofgren et al., 2008). However, neither a *Cyp2c* knockout nor a humanized CYP2C9 model has been described. The complex genetic organization of the mouse *Cyp2c* cluster, which is significantly larger and contains much more functional genes than any other *Cyp* gene cluster, could explain why such models have not been generated. Furthermore, CYP2C enzymes are expressed in the vascular epithelium and it has been speculated that enzymes such as CYP2C9 play important roles in angiogenesis, and vascular development (Michaelis et al., 2008; Webler et al., 2008). Therefore, the deletion of the *Cyp2c* cluster could potentially have deleterious effects both

Molecular Pharmacology Fast Forward. Published on August 23, 2012 as DOI: 10.1124/mol.112.080036
This article has not been copyedited and formatted. The final version may differ from this version.

during and subsequent to embryonic development.

Here we describe the generation of a *Cyp2c* cluster knockout (Cyp2c KO) mouse line, in which 14 of the 15 functional genes of this gene family have been deleted. Furthermore, we employed a sophisticated Cre-recombinase mediated insertion strategy in order to replace the mouse *Cyp2c* cluster with a liver-specific CYP2C9 expression cassette. Both the Cyp2c KO and the humanized CYP2C9 (hCYP2C9) mouse line were viable and fertile but showed certain phenotypic alterations in the liver. The initial characterization of these mouse lines is described, as well as the changes in activity towards selected CYP2C9 probe substrates.

Molecular Pharmacology Fast Forward. Published on August 23, 2012 as DOI: 10.1124/mol.112.080036
This article has not been copyedited and formatted. The final version may differ from this version.

Materials and Methods

Animal husbandry. Mice were kept as described previously (Scheer et al., 2008).

DNA constructs and cloning. For targeting the *Cyp2c55* gene locus a basic vector containing a Neomycin expression cassette, a *loxP* and *f3* site was constructed in pBluescript (pBS). In case of the Neomycin cassette the translational start ATG and the corresponding promoter is separated from an ATG-deficient Neomycin (5'Δ Neo) in frame by the *loxP* site, such that additional amino acids encoded by the *loxP* site are fused to the N-terminus of Neomycin. This constellation gives rise to a functional protein resulting in G418 resistance upon expression (Hasegawa et al., 2011). A 5.4 kb genomic sequence immediately upstream from the translational start site of the mouse *Cyp2c55* gene and a 3.0 kb fragment comprising exons 2 and 3 of *Cyp2c55*, both used as targeting arms for homologous recombination, were obtained by red/ET recombineering (Zhang et al., 1998) and subcloned into the basic targeting vector as depicted in Fig. 1C.

For targeting the *Cyp2c70* gene locus a basic vector containing thymidine kinase and hygromycine expression cassettes, a *loxP*, *lox5171* and *frt* site was constructed in pBluescript (pBS). A 5.5 kb genomic sequence comprising exons 7 and 8 of the mouse *Cyp2c70* gene and a 3.1 kb fragment comprising exons 4 and 5 of *Cyp2c70*, both used as targeting arms for homologous recombination, were obtained by red/ET recombineering and subcloned into the basic targeting vector as depicted in Fig. 1C.

Generation and molecular characterization of targeted embryonic stem cells. Culture and targeted mutagenesis of embryonic stem (ES cells) were carried out as described previously (Hogan et al., 1994). Details on the generation and molecular characterization of ES cell clones targeted at *Cyp2c55* and *Cyp2c70* gene loci are described in the Supplementary Materials and Methods.

Molecular Pharmacology Fast Forward. Published on August 23, 2012 as DOI: 10.1124/mol.112.080036
This article has not been copyedited and formatted. The final version may differ from this version.

Generation and molecular characterization of Cyp2c knockout and CYP2C9 humanized mice. For the generation of Cyp2c KO and hCYP2C9 mice, ES cell clones with a deletion of the *Cyp2c* cluster and an insertion of the human CYP2C9 expression cassette, respectively, were expanded, injected into BALBc-blastocysts and transferred into foster mothers as described previously (Hogan et al., 1994). Litters from these fosters were inspected visually and chimerism was determined by hair colour. Highly chimeric animals were used for breeding with either C57BL/6 WT mice (Cyp2c KO) or to an efficient flipase (Flpe) deleter strain carrying a transgene that expresses Flpe in the germ line (hCYP2C9). The latter approach led to a deletion of the neomycin expression cassette in the offspring (Fig. 1H). The Flpe-deleter strains was generated in house on a C57BL/6 genetic background. A detailed description on the molecular characterization of the Cyp2c KO and hCYP2C9 mice is given in the Supplementary Materials and Methods.

Animal experimentation. All animal procedures were carried out under a United Kingdom Home Office license, and all animal studies were approved by the Ethical Review Committee, University of Dundee. Homozygous mice for each transgenic line were used for experimental studies. C57BL/6 animals of the same age purchased from Harlan Olac (UK) were used as WT controls. All housing conditions were as described previously (Scheer et al., 2012).

Terminal procedures. Mice were killed by exposure to a rising concentration of CO_2 and blood was collected by cardiac puncture into lithium/heparin coated tubes for plasma preparation. Details on the procedures of tissue preparation, immunoblot analysis of Cyp2c and CYP2C9 protein expression, quantitative Reverse Transcriptase-PCR and in vitro and in vivo determination of CYP2C-dependent activities are described in the Supplementary Materials and Methods.

Molecular Pharmacology Fast Forward. Published on August 23, 2012 as DOI: 10.1124/mol.112.080036
This article has not been copyedited and formatted. The final version may differ from this version.

Results

Generation of CYP2C9 humanized and *Cyp2c* cluster knockout mice. The strategy of generating CYP2C9 humanized (hCYP2C9) and *Cyp2c* cluster knockout (Cyp2c KO) mice is illustrated in Fig. 1. The mouse *Cyp2c* cluster with the exception of *Cyp2c44*, which is located 4Mb away, was flanked with Cre recombinase recognition (*loxP*) sites using two consecutive rounds of targeting in mouse embryonic stem (ES) cells (Fig. 1A-D). Subsequent Cre-mediated recombination between the *loxP* sites resulted in a deletion of all exons and introns of *Cyp2c55*, *Cyp2c65*, *Cyp2c66*, *Cyp2c29*, *Cyp2c38*, *Cyp2c39*, *Cyp2c67*, *Cyp2c68*, *Cyp2c40*, *Cyp2c69*, *Cyp2c37*, *Cyp2c54* and *Cyp2c50*, as well as a deletion of exons 7-9 of *Cyp2c70* (Fig.1 E). The *Cyp2c* deleted ES cells were used to derive Cyp2c KO mice.

hCYP2C9 mice were generated from the *Cyp2c* deleted ES cells described above by further Cre-mediated insertion of an expression cassette in which human CYP2C9 is under control of the liver specific mouse albumin promoter (Fig. 1F). Cre-mediated insertion of this expression cassette was achieved by recombination via the *loxP* site that resulted from deletion of the mouse *Cyp2c* cluster and a heterospecific *lox5171* site (Lee and Saito, 1998) which was co-inserted with the *Cyp2c70* targeting vector (Fig. 1G). A neomycin complementation approach was used to achieve high stringency for the selection of ES cell clones with a correct Cre-mediated insertion (Hasegawa et al., 2011). In order to terminate any potential transcription from the *Cyp2c55* or *Cyp2c70* promoters, a polyA motif and a splice acceptor polyA motif were included upstream of the albumin promoter and downstream of the CYP2C9 expression cassette, respectively. Transgenic mice from correctly targeted ES cells were generated subsequently and by further crosses with a mouse line expressing the Flp-recombinase in the germ line the neomycin expression cassette was deleted via recombination at the Flp recombinase recognition (*frt*) sites (Fig. 1H). Homozygous hCYP2C9 and Cyp2c KO mice were obtained by breeding.

Molecular Pharmacology Fast Forward. Published on August 23, 2012 as DOI: 10.1124/mol.112.080036
This article has not been copyedited and formatted. The final version may differ from this version.

Phenotypic characterization of CYP2C9 humanized and *Cyp2c* cluster knockout mice. Homozygous humanized and knockout mice appeared normal, could not be distinguished from WT animals and had normal body weights, liver weights and fertility (data not shown). In order to further characterize the hCYP2C9 and Cyp2c KO mice, plasma samples were analysed for albumin, alkaline phosphatase, alanine amino transferase, aspartate aminotransferase, direct and total bilirubin, high and low density lipoproteins, triglycerides and cholesterol (n=3 mice per line). The only significant phenotypic change in the hCYP2C9 mice was a ~0.5-fold decrease in alkaline phosphatase activity. The Cyp2c KO mice exhibited a similar change and also a small but significant decrease (~0.7-fold) in high density lipoprotein and cholesterol (Supplementary Fig.1). Alanine amino transferase and aspartate aminotransferase activities were also increased in both genetically modified mouse lines, but the variability between individual mice were high and the changes were not statistically significant. In order to assess if the increased alanine amino transferase and aspartate aminotransferase activities may indicate hepatotoxicity, we carried out a haematoxylin and eosin analysis on livers of hCYP2C9 and Cyp2c KO mice. Compared to WT controls this analysis indeed showed an increased infiltration by lymphocytes and neutrophils and unidentified 'ovoid' cells in the portal areas of samples from both the Cyp2cKO and hCYP2C9 mice (Supplementary Fig.2). The degree of this pathology was variable between samples.

Human CYP2C9 and mouse Cyp2c expression in Cyp2c KO and CYP2C9 humanized mice. The expression of human *CYP2C9* mRNA in the liver of WT, Cyp2c KO and hCYP2C9 mice was determined by TaqMan analysis. This confirmed the expression of *CYP2C9* in the hCYP2C9 model (Fig. 2A). The average Ct value of 21.8 (n=3 mice) for *CYP2C9* mRNA in the hCYP2C9 mice was comparable to many hepatic mouse cytochrome P450 genes. The *CYP2C9* mRNA level in other organs was negligible (data not shown). For

Molecular Pharmacology Fast Forward. Published on August 23, 2012 as DOI: 10.1124/mol.112.080036
This article has not been copyedited and formatted. The final version may differ from this version.

example, the average Ct value for *CYP2C9* in the duodenum was 29.0, i.e. at the limit of detection. The loss of hepatic mouse *Cyp2c* mRNA expression in the Cyp2c KO and hCYP2C9 models was confirmed through the finding that the mRNAs for the three distant mouse *Cyp2c* genes *Cyp2c55*, *Cyp2c39* and *Cyp2c70* could be readily detected in WT animals, but not in homozygous Cyp2c KO and hCYP2C9 mice (Fig. 2B). No significant changes in the expression of the remaining mouse *Cyp2c* gene *Cyp2c44* was measured in either the Cyp2c KO or hCYP2C9 animals (Fig. 2C).

In order to analyse the expression of CYP2C proteins in the liver of WT, Cyp2c KO and hCYP2D9 mice, microsomes from these three mouse lines were studied by Western blotting. Using a mouse Cyp2c specific antibody, immunoreactive *Cyp2c* proteins were detected in WT but not in Cyp2c KO or hCYP2C9 mice, confirming the loss of mouse Cyp2c protein expression in these transgenic mouse lines (Fig. 2D). Using a human-specific CYP2C9/19 antibody, CYP2C9 was only detected in liver microsomes from hCYP2C9 mice (Fig. 2D), the level of expression being comparable to that detected in human liver microsomes.

Cytochrome P450-mediated catalytic activity in WT, Cyp2c KO and hCYP2C9 mice. In Cyp2c KO mice tolbutamide methylhydroxylase activity, a prototypical CYP2C substrate, was markedly decreased (91%) compared to WT controls, suggesting that murine Cyp2c proteins play a major role in the metabolism of this compound in mice (Fig. 3A). Tolbutamide methylhydroxylase activity in microsomes from the hCYP2C9 mice was significantly higher that in mice nulled for the Cyp2c proteins (4.5-fold), demonstrating that the CYP2C9 protein is catalytically active. The tolbutamide methylhydroxylase activity of human liver microsomes (HLM) was in between that of WT and hCYP2C9 mice.

Diclofenac 4-hydroxylation in hCYP2C9 mice was comparable to human liver microsomes and was significantly higher than for WT and Cyp2c KO animals (Fig. 3B). The ~2-fold

Molecular Pharmacology Fast Forward. Published on August 23, 2012 as DOI: 10.1124/mol.112.080036
This article has not been copyedited and formatted. The final version may differ from this version.

higher activity in hCYP2C9 humanized compared to Cyp2c KO mice further confirmed the functionality of the CYP2C9 protein in the hCYP2C9 mouse line. Interestingly, diclofenac 4-hydroxylase activity was similar in WT and Cyp2c KO mice, indicating that diclofenac is not a major substrate of the deleted mouse Cyp2c enzymes.

In vivo pharmacokinetics of tolbutamide in WT, Cyp2c KO and CYP2C9 humanized mice. The pharmacokinetics of tolbutamide was determined in WT, Cyp2c KO and hCYP2C9 mice. Over a time period of 8 hours, highest tolbutamide levels were observed in Cyp2c KO animals, followed by hCYP2C9 and WT mice (n=3 mice per line) (Fig. 4A). Furthermore, compared to WT controls the tolbutamide area under concentration versus time curve (AUC) was significantly increased by ~1.6-fold in Cyp2c KO mice (Fig. 4B). hCYP2C9 mice showed an ~1.25-fold higher AUC than WT animals, but this change was not statistically significant. Overall, the pharmacokinetics of tolbutamide in these three mouse lines was in agreement with the in vitro results and confirmed the contribution of the mouse Cyp2c enzymes and human CYP2C9 in the metabolism of this compound in vivo. It should be noted that signs of toxicity were observed in all three mouse lines at the tested dose level (5 mg/kg, ip), so that it was decided to terminate the study at 8 hours after administration of tolbutamide. Conclusions from the in vivo study therefore need to be drawn with caution.

Inhibition of tolbutamide hydroxylation in WT, Cyp2c KO and hCYP2C9 mice. The effect of different CYP2C inhibitors on the hydroxylation of tolbutamide was determined using liver microsomes from WT, Cyp2c KO and hCYP2C9 mice, and the results were compared with the inhibition observed in human liver microsomes. At the concentrations used fluvoxamine, fluoxetine and fluconazole strongly inhibited tolbutamide methylhydroxylase activity in microsomes from WT mice by >75%, but with 14-40% inhibition the effect in samples from hCYP2C9 mice or human liver was much smaller (Fig. 6A-C). Interestingly, some minor inhibition in liver microsomes from Cyp2c KO mice was also observed with

Molecular Pharmacology Fast Forward. Published on August 23, 2012 as DOI: 10.1124/mol.112.080036
This article has not been copyedited and formatted. The final version may differ from this version.

fluvoxamine and fluoxetine, indicating that other enzymes might be involved. In contrast, sulfaphenazole and benzbromarone strongly inhibited the hydroxylation of tolbutamide in hepatic microsomal samples from hCYP2C9 mice and humans by 60-90%, but had no effect on this reaction in microsomes from WT or Cyp2c KO mice (Fig. 6D-E). In summary, the activity of the inhibitors in samples of the hCYP2C9 mice was in good agreement with those from human liver microsomes.

Compensatory changes in the expression of other drug metabolising enzymes in Cyp2c KO and CYP2C9 humanized mice. The deletion of cytochrome P450 genes in the mouse can result in compensatory changes in other pathways of drug metabolism (van Waterschoot et al., 2008) We therefore compared the mRNA levels of a selected number of genes coding for key mouse drug metabolising enzymes by qRT-PCR analysis (n=3 mice per line). Compared to the WT controls, no significant changes in any of the hepatic cytochrome P450 genes analysed (*Cyp3a11*, *Cyp3a13*, *Cyp2d9*, *Cyp2d22* and *Cyp2d26*) were observed in hCYP2C9 or Cyp2c KO mice (Fig. 5). However, moderate but statistically significant decreases in the hepatic mRNA expression levels of *Ugt1a6* (0.7 and 0.6-fold), *Ugt2b5* (0.6 and 0.7-fold) and *Ugt2b34* (0.6 and 0.6-fold) were found in hCYP2C9 and Cyp2c KO mice, respectively. No significant changes in the expression of any of these genes were observed in the intestine of the two transgenic mouse lines (data not shown).

Molecular Pharmacology Fast Forward. Published on August 23, 2012 as DOI: 10.1124/mol.112.080036
This article has not been copyedited and formatted. The final version may differ from this version.

Discussion

CYP2C9 plays a major role in the metabolic clearance of many important classes of therapeutic drugs, such as nonsteroidal antiinflammatories, oral anticoagulants and oral hypoglycemics. Furthermore, it is one of the most abundant cytochrome P450 enzymes expressed in human liver and pharmacological inhibition or pharmacogenetic variability of CYP2C9 can be associated with severe adverse drug reactions (Rettie and Jones, 2005).

In this report we have generated a model which can be used to study the in vivo consequences of CYP2C9-mediated drug metabolism and drug-drug interactions. The value of traditional preclinical animal models for such studies is compromised, due to the significant species differences in the multiplicity and substrate specificity of CYP2C enzymes (Baillie and Rettie, 2011; Nelson et al., 2004). Although humanized and knockout mouse models for other major drug metabolising enzymes have been developed recently (Cheung et al., 2005; Cheung et al., 2006; Corchero et al., 2001; Dragin et al., 2007; Hasegawa et al., 2011; Jiang et al., 2005; Lofgren et al., 2008; Scheer et al., 2012; van Herwaarden et al., 2007), this is the first report of a humanized CYP2C9 or a *Cyp2c* knockout mouse model . In order to create these mice the significant technical challenge and biological risk of deleting the very large mouse *Cyp2c* cluster needed to be overcome.

To this end a sophisticated combination of homologous recombination, Cre-mediated deletion and Cre-mediated targeted insertion was applied. Both the hCYP2C9 and the Cyp2c KO mice were viable and fertile and did not display any visual physiological abnormalities, suggesting that the deleted mouse *Cyp2c* genes have no vitally important role during development. This observation was further sustained by the fact that compared to WT controls no changes in body and liver weights and most clinical chemistry parameters were detected in the transgenic animals. However, ~50% decreased alkaline phosphatase activities were observed in

Molecular Pharmacology Fast Forward. Published on August 23, 2012 as DOI: 10.1124/mol.112.080036
This article has not been copyedited and formatted. The final version may differ from this version.

hCYP2C9 and Cyp2c KO mice, as well as small, but statistically significant decreases in high density lipoproteins and cholesterol in the Cyp2c KO model. These changes are presumably a consequence of the deletion of the mouse *Cyp2c* genes. For example, changes in alkaline phosphatise activities can be associated with the levels of different vitamins, such as vitamin B6, B12, C or D (Aasheim et al., 2008; Faiz et al., 2007), and it is known that cytochrome P450 enzymes can be involved in vitamin metabolism (Guengerich, 2003). On the other hand, we can not rule out the possibility that the observed differences are caused by subtle variations in the genetic background of the mouse strains used in the experiments. Sequence polymorphisms in the alkaline phosphatase 2 gene have been found between different mouse strains, which are associated with differences in alkaline phosphatase levels (Foreman et al., 2005). However, this explanation appears unlikely due to the fact that all mouse lines used in our studies were on a consistent C57BL/6 genetic background. In addition to the changes described above, the average alanine amino transferase and aspartate aminotransferase activities were higher in both genetically modified mouse lines than in WT animals. This result is in agreement with the liver pathology observed by haematoxylin and eosin analysis in both transgenic models. The fact that the changes observed in the hCYP2C9 mice were also visible in the Cyp2c KO animals indicates that these effects reflect roles of the mouse Cyp2c enzymes in endogenous processes and that they are not a consequence of the expression of human CYP2C9. The Cyp2c KO model should facilitate studies to assess these roles.

Human CYP2C9 was expressed in the liver of the hCYP2C9 mice at levels similar to those found in human liver. Furthermore, the enzyme was active in the hydroxylation of the two established CYP2C9 probe substrates tolbutamide and dicolfenac. Tolbutamide methylhydroxylase activity was higher in WT mice than in hCYP2C9 mice, suggesting that tolbutamide is a preferred substrate of the mouse Cyp2c enzymes. In contrast, diclofenac 4-hydroxylation was higher in the hCYP2C9 samples. The fact that the deletion of the mouse

Molecular Pharmacology Fast Forward. Published on August 23, 2012 as DOI: 10.1124/mol.112.080036
This article has not been copyedited and formatted. The final version may differ from this version.

Cyp2c cluster did not result in a reduction in diclofenac 4-hydroxylation demonstrates that either the murine Cyp2c enzymes are not active towards this substrate or that there is a compensatory increase in other P450s active in its metabolism. This result might be explained by previous observations in rats indicating that the metabolic activation of diclofenac through oxidation is catalysed not only by Cyp2c, but also Cyp2b and Cyp3a enzymes (Tang et al., 1999).

One potential use of the hCYP2C9 model is for CYP2C9 inhibition studies, for example to predict drug-drug interactions in humans. To this end we tested the effect of a number of CYP2C inhibitors on the hydroxylation of tolbutamide in liver microsomes from WT, Cyp2c KO and hCYP2C9 mice and compared the results with those obtained from human liver microsomes. While a clear difference was observed between samples from WT mice and humans, the hCYP2C9 model reliably predicted the inhibition of activity seen in human liver microsomes.

In a previous report the deletion of the mouse *Cyp3a* gene cluster was associated with considerable compensatory changes in other gene families involved in drug metabolism and disposition (van Waterschoot et al., 2009; van Waterschoot et al., 2008). For the limited number of genes analysed in the present study, only some small reductions in the expression of different *Ugt* genes were measured in the Cyp2c KO mice which were not reversed in the hCYP2C9 model. This is in contrast to the Cyp3a knockout model where the increased expression of, for example, *Cyp2c55* was reversed when a transgene expressing CYP3A4 was expressed in the liver (van Waterschoot et al., 2009). The effect of the deletion of the mouse *Cyp2c* cluster on the expression of other genes not analysed in the present work needs to be assessed by further studies.

Cytochrome P450 humanized mouse models provide a powerful approach to overcome the

Molecular Pharmacology Fast Forward. Published on August 23, 2012 as DOI: 10.1124/mol.112.080036
This article has not been copyedited and formatted. The final version may differ from this version.

species differences in drug metabolism (Gonzalez and Yu, 2006). In the new model CYP2C9 is expressed off the albumin promoter, which implies that it should be expressed throughout the liver acinus whereas Cyp2c proteins are expressed in centrilobular hepatocytes. We have attempted to carry out immunohistochemistry to compare Cyp2c/CYP2C9 protein expression in hCYP2C9 and WT mice, but to date these experiments have been unsuccessful. Furthermore, due to the use of the albumin promoter the expression of CYP2C9 is not inducible by exogenous chemicals as it has been shown to be in humans (Al-Dosari et al., 2006; Chen et al., 2004; Ferguson et al., 2002; Gerbal-Chaloin et al., 2002). Finally, in man CYP2C9 is expressed in the intestine (Paine et al., 2006), which is not the case in the hCYP2C9 model and the observed liver pathology may complicate the use of the model for certain applications. These points should be taken into account when interpreting data using this model. Despite these limitations, the novel hCYP2C9 and Cyp2c KO mice provide valuable models for evaluating the role of this enzyme in the metabolism and disposition of drugs and foreign compounds; for example, to assess the role of CYP2C9 in systemic drug clearance, for CYP2C9 inhibition studies or, relating to regulatory guidance, for the identification and safety assessment of CYP2C9 metabolites (Powley et al., 2009). Furthermore, it was recently shown that the mouse Cyp2c enzymes play an important role in the metabolism of substrates which are otherwise metabolised by CYP3A4 in humans. For example, the mouse Cyp2c enzymes significantly contributed to the in vivo metabolism of midazolam, a highly specific CYP3A4 substrate in humans (van Waterschoot et al., 2008). Therefore, the combination of the hCYP2C9 model with one of the previously described CYP3A4 humanized mouse lines (Hasegawa et al., 2011; van Herwaarden et al., 2007), might help to overcome the background effects of mouse Cyp2c enzymes on the metabolism of CYP3A4 substrates.

Molecular Pharmacology Fast Forward. Published on August 23, 2012 as DOI: 10.1124/mol.112.080036
This article has not been copyedited and formatted. The final version may differ from this version.

Acknowledgements

We wish to thank Vincent Beuger, Lisa Antoni, Sylvia Krueger and Anja Mueller (TaconicArtemis, Cologne), Barbara Elcombe, Marie Bowers, Lori Woods, Corinne Haines, Nick Birse and Sol Gibson (CXR Biosciences, Dundee) and Colin Henderson (University of Dundee) for technical assistance.

Molecular Pharmacology Fast Forward. Published on August 23, 2012 as DOI: 10.1124/mol.112.080036
This article has not been copyedited and formatted. The final version may differ from this version.

Authorship Contributions

Participated in research design: Scheer, Kapelyukh, Wolf

Conducted experiments: Rode, Buechel, Kapelyukh, Chatham

Performed data analysis: Scheer, Kapelyukh, Wolf

Wrote or contributed to the writing of the manuscript: Scheer, Kapelyukh, Wolf

Molecular Pharmacology Fast Forward. Published on August 23, 2012 as DOI: 10.1124/mol.112.080036
This article has not been copyedited and formatted. The final version may differ from this version.

References

Aasheim ET, Hofso D, Hjelmesaeth J, Birkeland KI and Bohmer T (2008) Vitamin status in morbidly obese patients: a cross-sectional study. *Am J Clin Nutr* **87**(2):362-369.

Al-Dosari MS, Knapp JE and Liu D (2006) Activation of human CYP2C9 promoter and regulation by CAR and PXR in mouse liver. *Mol Pharm* **3**(3):322-328.

Baillie TA and Rettie AE (2011) Role of biotransformation in drug-induced toxicity: influence of intra- and inter-species differences in drug metabolism. *Drug Metab Pharmacokinet* **26**(1):15-29.

Chen Y, Ferguson SS, Negishi M and Goldstein JA (2004) Induction of human CYP2C9 by rifampicin, hyperforin, and phenobarbital is mediated by the pregnane X receptor. *J Pharmacol Exp Ther* **308**(2):495-501.

Cheung C, Ma X, Krausz KW, Kimura S, Feigenbaum L, Dalton TP, Nebert DW, Idle JR and Gonzalez FJ (2005) Differential metabolism of 2-amino-1-methyl-6-phenylimidazo[4,5-b]pyridine (PhIP) in mice humanized for CYP1A1 and CYP1A2. *Chem Res Toxicol* **18**(9):1471-1478.

Cheung C, Yu AM, Chen CS, Krausz KW, Byrd LG, Feigenbaum L, Edwards RJ, Waxman DJ and Gonzalez FJ (2006) Growth hormone determines sexual dimorphism of hepatic cytochrome P450 3A4 expression in transgenic mice. *J Pharmacol Exp Ther* **316**(3):1328-1334.

Corchero J, Granvil CP, Akiyama TE, Hayhurst GP, Pimprale S, Feigenbaum L, Idle JR and Gonzalez FJ (2001) The CYP2D6 humanized mouse: effect of the human CYP2D6 transgene and HNF4alpha on the disposition of debrisoquine in the mouse. *Mol Pharmacol* **60**(6):1260-1267.

Dragin N, Uno S, Wang B, Dalton TP and Nebert DW (2007) Generation of 'humanized' hCYP1A1_1A2_Cyp1a1/1a2(-/-) mouse line. *Biochem Biophys Res Commun* **359**(3):635-642.

Faiz S, Panunti B and Andrews S (2007) The epidemic of vitamin D deficiency. *J La State Med Soc* **159**(1):17-20; quiz 20, 55.

Ferguson SS, LeCluyse EL, Negishi M and Goldstein JA (2002) Regulation of human CYP2C9 by the constitutive androstane receptor: discovery of a new distal binding site. *Mol Pharmacol* **62**(3):737-746.

Foreman JE, Blizard DA, Gerhard G, Mack HA, Lang DH, Van Nimwegen KL, Vogler GP, Stout JT, Shihabi ZK, Griffith JW, Lakoski JM, McClearn GE and Vandenbergh DJ (2005) Serum alkaline phosphatase activity is regulated by a chromosomal region containing the alkaline phosphatase 2 gene (Akp2) in C57BL/6J and DBA/2J mice. *Physiol Genomics* **23**(3):295-303.

Gerbal-Chaloin S, Daujat M, Pascussi JM, Pichard-Garcia L, Vilarem MJ and Maurel P (2002) Transcriptional regulation of CYP2C9 gene. Role of glucocorticoid receptor and constitutive androstane receptor. *J Biol Chem* **277**(1):209-217.

Gonzalez FJ and Yu AM (2006) Cytochrome P450 and xenobiotic receptor humanized mice. *Annu Rev Pharmacol Toxicol* **46**:41-64.

Guengerich FP (2003) Cytochromes P450, drugs, and diseases. *Mol Interv* **3**(4):194-204.

Guengerich FP (2008) Cytochrome p450 and chemical toxicology. *Chem Res Toxicol* **21**(1):70-83.

Hasegawa M, Kapelyukh Y, Tahara H, Seibler J, Rode A, Krueger S, Lee DN, Wolf CR and Scheer N (2011) Quantitative prediction of human pregnane X receptor and cytochrome P450 3A4 mediated drug-drug interaction in a novel multiple humanized mouse line. *Mol Pharmacol* **80**(3):518-528.

Hogan BLM, Beddington RSP, Costantini F and Lacy E (1994) in *Manipulating the Mouse*

Molecular Pharmacology Fast Forward. Published on August 23, 2012 as DOI: 10.1124/mol.112.080036
This article has not been copyedited and formatted. The final version may differ from this version.

Embryo: A Laboratory Manual pp 253-289, Cold Spring Harbor Lab. Press, Plainview, New York.

Jiang Z, Dalton TP, Jin L, Wang B, Tsuneoka Y, Shertzer HG, Deka R and Nebert DW (2005) Toward the evaluation of function in genetic variability: characterizing human SNP frequencies and establishing BAC-transgenic mice carrying the human CYP1A1_CYP1A2 locus. *Hum Mutat* **25(**2):196-206.

Lofgren S, Baldwin RM, Hiratsuka M, Lindqvist A, Carlberg A, Sim SC, Schulke M, Snait M, Edenro A, Fransson-Steen R, Terelius Y and Ingelman-Sundberg M (2008) Generation of mice transgenic for human CYP2C18 and CYP2C19: characterization of the sexually dimorphic gene and enzyme expression. *Drug Metab Dispos* **36**(5):955-962.

Michaelis UR, Xia N, Barbosa-Sicard E, Falck JR and Fleming I (2008) Role of cytochrome P450 2C epoxygenases in hypoxia-induced cell migration and angiogenesis in retinal endothelial cells. *Invest Ophthalmol Vis Sci* **49**(3):1242-1247.

Nelson DR, Zeldin DC, Hoffman SM, Maltais LJ, Wain HM and Nebert DW (2004) Comparison of cytochrome P450 (CYP) genes from the mouse and human genomes, including nomenclature recommendations for genes, pseudogenes and alternative-splice variants. *Pharmacogenetics* **14**(1):1-18.

Paine MF, Hart HL, Ludington SS, Haining RL, Rettie AE and Zeldin DC (2006) The human intestinal cytochrome P450 "pie". *Drug Metab Dispos* **34**(5):880-886.

Powley MW, Frederick CB, Sistare FD and DeGeorge JJ (2009) Safety assessment of drug metabolites: implications of regulatory guidance and potential application of genetically engineered mouse models that express human P450s. *Chem Res Toxicol* **22**(2):257-262.

Rettie AE and Jones JP (2005) Clinical and toxicological relevance of CYP2C9: drug-drug interactions and pharmacogenetics. *Annu Rev Pharmacol Toxicol* **45**:477-494.

Scheer N, Kapelyukh Y, McEwan J, Beuger V, Stanley LA, Rode A and Wolf CR (2012) Modeling human cytochrome P450 2D6 metabolism and drug-drug interaction by a novel panel of knockout and humanized mouse lines. *Mol Pharmacol* **81**(1):63-72.

Scheer N, Ross J, Rode A, Zevnik B, Niehaves S, Faust N and Wolf CR (2008) A novel panel of mouse models to evaluate the role of human pregnane X receptor and constitutive androstane receptor in drug response. *J Clin Invest* **118**(9):3228-3239.

Stubbins MJ, Harries LW, Smith G, Tarbit MH and Wolf CR (1996) Genetic analysis of the human cytochrome P450 CYP2C9 locus. *Pharmacogenetics* **6**(5):429-439.

Tang W, Stearns RA, Bandiera SM, Zhang Y, Raab C, Braun MP, Dean DC, Pang J, Leung KH, Doss GA, Strauss JR, Kwei GY, Rushmore TH, Chiu SH and Baillie TA (1999) Studies on cytochrome P-450-mediated bioactivation of diclofenac in rats and in human hepatocytes: identification of glutathione conjugated metabolites. *Drug Metab Dispos* **27**(3):365-372.

van Herwaarden AE, Wagenaar E, van der Kruijssen CM, van Waterschoot RA, Smit JW, Song JY, van der Valk MA, van Tellingen O, van der Hoorn JW, Rosing H, Beijnen JH and Schinkel AH (2007) Knockout of cytochrome P450 3A yields new mouse models for understanding xenobiotic metabolism. *J Clin Invest* **117**(11):3583-3592.

van Waterschoot RA, Rooswinkel RW, Wagenaar E, van der Kruijssen CM, van Herwaarden AE and Schinkel AH (2009) Intestinal cytochrome P450 3A plays an important role in the regulation of detoxifying systems in the liver. *FASEB J* **23**(1):224-231.

van Waterschoot RA, van Herwaarden AE, Lagas JS, Sparidans RW, Wagenaar E, van der Kruijssen CM, Goldstein JA, Zeldin DC, Beijnen JH and Schinkel AH (2008) Midazolam metabolism in cytochrome P450 3A knockout mice can be attributed to up-regulated CYP2C enzymes. *Mol Pharmacol* **73**(3):1029-1036.

Webler AC, Popp R, Korff T, Michaelis UR, Urbich C, Busse R and Fleming I (2008)

Cytochrome P450 2C9-induced angiogenesis is dependent on EphB4. *Arterioscler Thromb Vasc Biol* **28**(6):1123-1129.

Williams JA, Hyland R, Jones BC, Smith DA, Hurst S, Goosen TC, Peterkin V, Koup JR and Ball SE (2004) Drug-drug interactions for UDP-glucuronosyltransferase substrates: a pharmacokinetic explanation for typically observed low exposure (AUCi/AUC) ratios. *Drug Metab Dispos* **32**(11):1201-1208.

Zhang Y, Buchholz F, Muyrers JP and Stewart AF (1998) A new logic for DNA engineering using recombination in Escherichia coli. *Nat Genet* **20**(2):123-128.

Molecular Pharmacology Fast Forward. Published on August 23, 2012 as DOI: 10.1124/mol.112.080036
This article has not been copyedited and formatted. The final version may differ from this version.

Footnotes

Financial support:

Part of this work was supported by ITI Life Sciences, Scotland.

Reprint requests:

Nico Scheer, PhD, TaconicArtemis, Neurather Ring 1, 51063 Koeln, Germany.

Tel.: +49 221 9645343; Fax: +49 221 9645321; Email: nico.scheer@taconicartemis.com

Molecular Pharmacology Fast Forward. Published on August 23, 2012 as DOI: 10.1124/mol.112.080036
This article has not been copyedited and formatted. The final version may differ from this version.

Figure Legends

Fig. 1: Strategy for generating Cyp2c KO and hCYP2C9 mice. (A) Schematic representation of the chromosomal organization and orientation of functional genes within the mouse *Cyp2c* cluster. (B) Exon/Intron structure of *Cyp2c55* and *Cyp2c70*. Exons are represented as black bars and the ATGs mark the translational start sites of both genes. The positions of the targeting arms for homologous recombination are highlighted in grey (*Cyp2c55*) and black (*Cyp2c70*), respectively. (C) Vectors used for targeting of *Cyp2c55* (left) and *Cyp2c70* (right) by homologous recombination. *LoxP*, *lox5171*, *frt* and *f3* sites are represented as white, stripped, black and grey triangles, respectively. (D) Genomic organization of the *Cyp2c* cluster in double targeted ES cells after insertion of the targeting vectors. (E) Deletion of the mouse *Cyp2c* cluster after Cre-mediated recombination at the *loxP* sites. (F) CYP2C9 expression cassette used for Cre-mediated insertion via the *loxP* and *lox5171* sites. (G) Mouse *Cyp2c* locus after Cre-mediated insertion of the CYP2C9 expression cassette. (H) Mouse *Cyp2c* locus in the hCYP2C9 model after Flp-mediated deletion of the neomycin expression cassette. For the sake of clarity sequences are not drawn to scale. Hyg = Hygromycin expression cassette, TK = thymidine kinase expression cassette, alb Prom = mouse albumin enhancer/promoter element, P = Promoter that drives the expression of neomycin, 5'Δ Neo = ATG-deficient neomycin.

Fig. 2: Analysis of Cyp2c and CYP2C9 expression in WT, Cyp2c KO and hCYP2C9 mice. (A) Relative expression levels of human *CYP2C9*, (B) mouse *Cyp2c39*, *Cyp2c55*, *Cyp2c70* and (C) mouse *Cyp2c44* mRNA in the liver of WT, Cyp2c KO and hCYP2C9 mice. Expression levels in hCYP2C9 mice (in case of *CYP2C9* mRNA) and in WT animals (in case

Molecular Pharmacology Fast Forward. Published on August 23, 2012 as DOI: 10.1124/mol.112.080036
This article has not been copyedited and formatted. The final version may differ from this version.

of *Cyp2c39*, *Cyp2c55*, *Cyp2c70* and *Cyp2c44* mRNA) were arbitrarily set as one. Data are expressed as Mean ± SD (n=3 mice per genotype). Transgenic mice were compared with WT animals using a Student's t-test (2-sided), with * and ** statistically different from control at <0.05 and <0.01, respectively. (D) Mouse Cyp2c (upper lane) and human CYP2C9 (lower lane) protein expression in liver microsomes from WT, Cyp2c KO and hCYP2C9 mice shown by Western blot analysis using a mouse-specific monoclonal anti-Cyp2c or a human-specific CYP2C9/19 antibody, respectively. The positive controls were recombinant CYP2C9 ($2C9^{rec}$) and human liver microsomes (HLM), respectively.

Fig. 3: In vitro metabolism of CYP2C9 probe substrates by liver microsomes from WT, Cyp2c KO and hCYP2C9 mice and humans. (A) Tolbutamide methylthydroxylation and (B) diclofenac 4'-hydroxylation. Data are expressed as Mean ± SD (n=3 for all mouse lines). Activities in samples from Cyp2c KO mice were compared to that from WT and hCYP2C9 mice using a Student's t-test (2-sided), with * and *** statistically different from these mouse lines at p<0.05 and <0.001, respectively. HLM = Human liver microsomes.

Fig. 4: Pharmacokinetics of tolbutamide in WT, Cyp2c KO and hCYP2C9 mice. (A) Concentration versus time profiles and (B) areas under the concentration versus time (0-8 hours) curves (AUC). Data are expressed as Mean ± SD (n=3 mice per genotype). AUCs for Cyp2c KO and hCYP2C9 mice were compared to WT controls using a Student's t-test (2-sided), with ** statistically different from controls at p<0.01.

Fig. 5: Hepatic mRNA expression levels of selected genes coding for drug metabolising

enzymes in WT, Cyp2c KO and hCYP2C9 mice. (A) Relative expression levels of mouse *Cyp3a11*, *Cyp3a13*, *Cyp2d9*, *Cyp2d22*, *Cyp2d26*, *Ugt1a6*, *Ugt2b5* and *Ugt2b34* mRNA in the liver of WT, Cyp2c KO and hCYP2C9 mice. Expression levels in WT animals were arbitrarily set as one. Data are expressed as Mean ± SD (n=3 mice per genotype). Transgenic mice were compared with WT animals using a Student's t-test (2-sided), with * and ** statistically different from control at <0.05 and <0.01, respectively.

Fig. 6: Inhibition of vitro metabolism of tolbutamide in liver microsomes from WT, Cyp2c KO and hCYP2C9 mice and humans. Tolbutamide methylhydroxylation either without inhibitor (black bars) or during co-incubation with (A) 2 µM fluvoxamine, (B) 15 µM fluoxetine, (C) 5 µM fluconazole, (D) 50 µM sulfaphenazole and (E) 0.25 µM benzbromarone (white bars). Tolbutamide concentration was 100 µM, microsomal protein concentration 0.5 mg/ml and incubation time 20 min in all experiments. Data are expressed as Mean ± SD (n=3 for all mouse lines). Activities of inhibitor treated samples were compared to that from the corresponding control group using a Student's t-test (2-sided), with *, ** and *** statistically different from control at p<0.05, p<0.01 and <0.001, respectively. HLM = Pooled human liver microsomes.

Figure 1

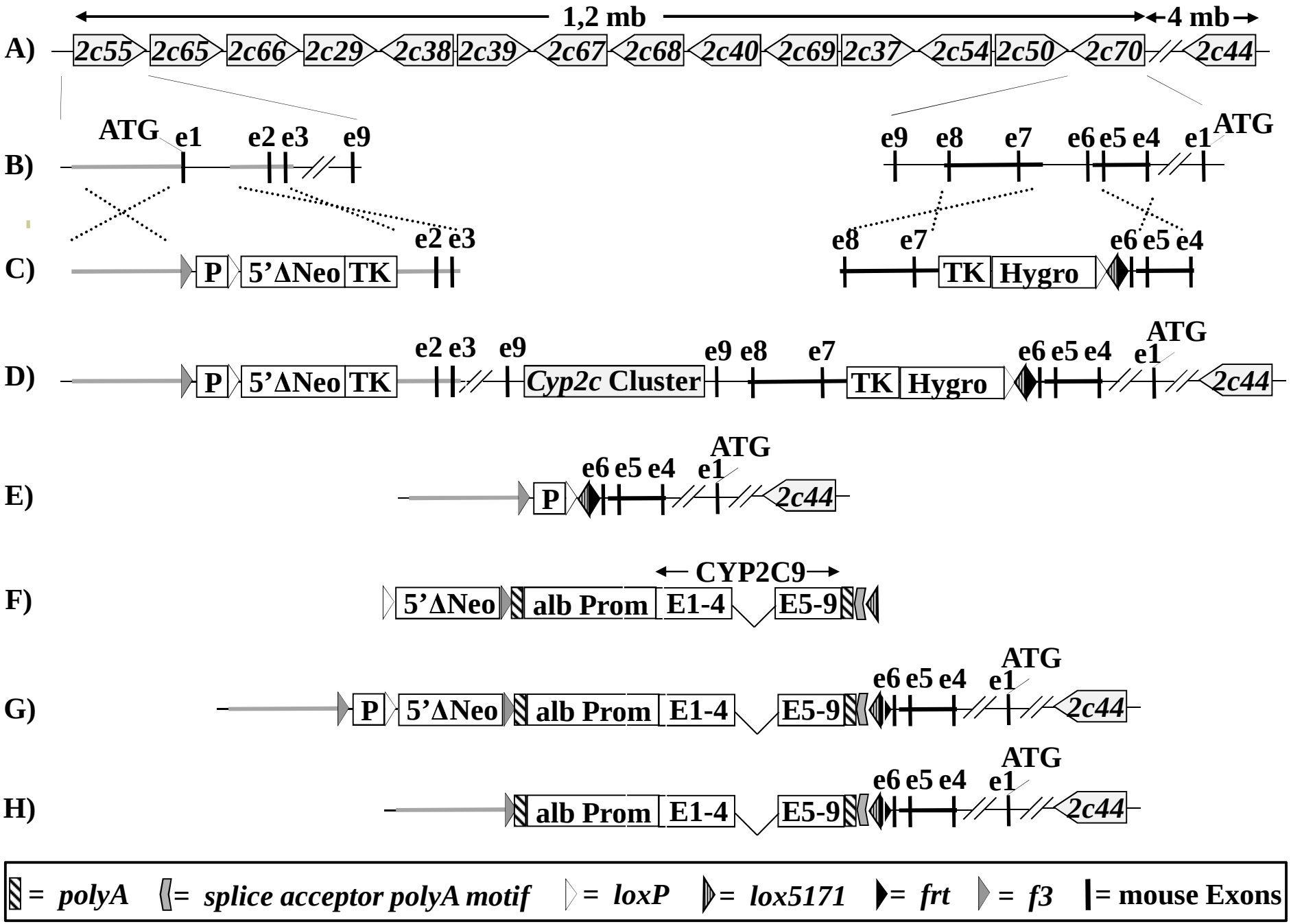

Figure 2

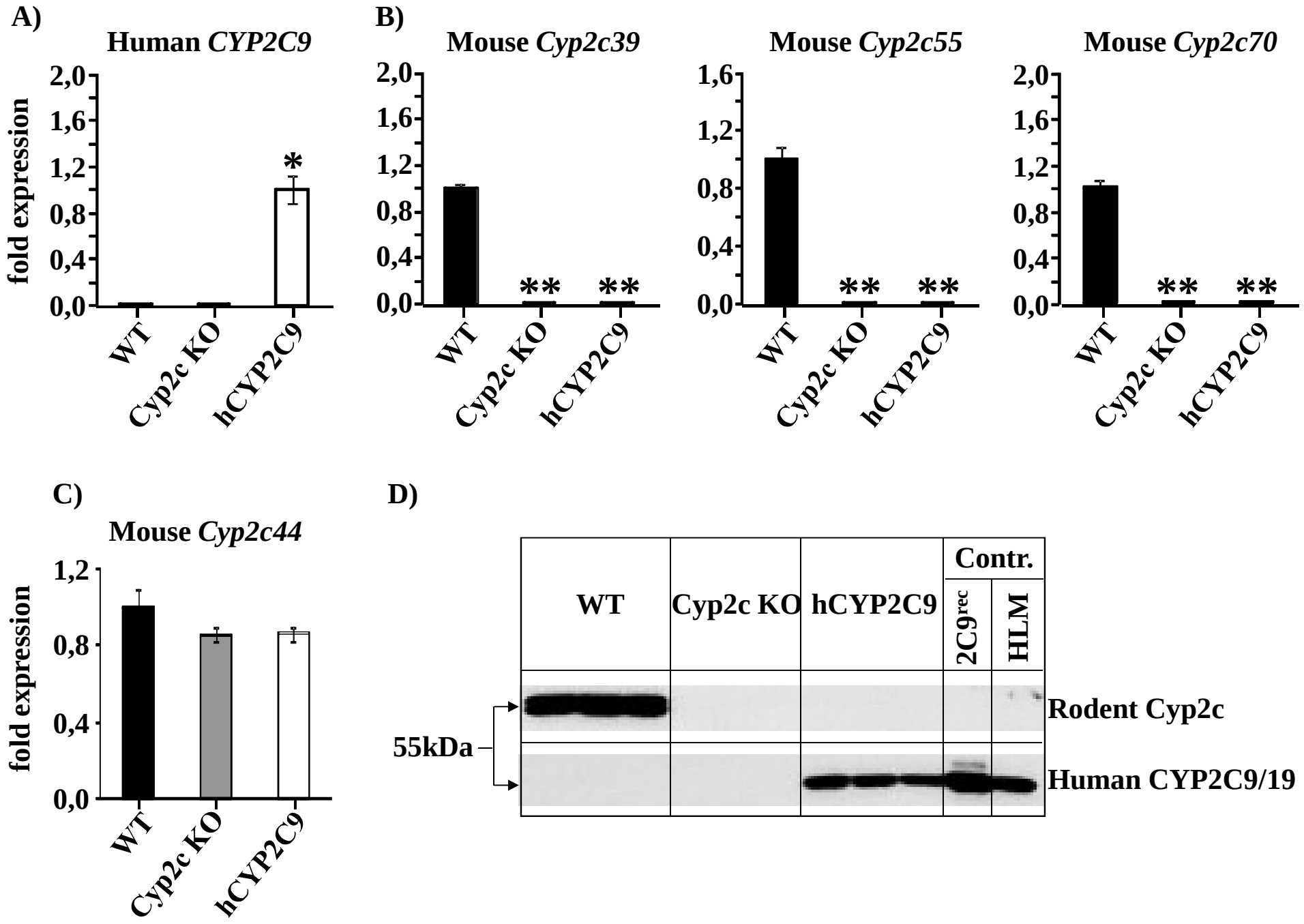

Molecular Pharmacology Fast Forward. Published on August 23, 2012 as DOI: 10.1124/mol.112.080036
This article has not been copyedited and formatted. The final version may differ from this version.

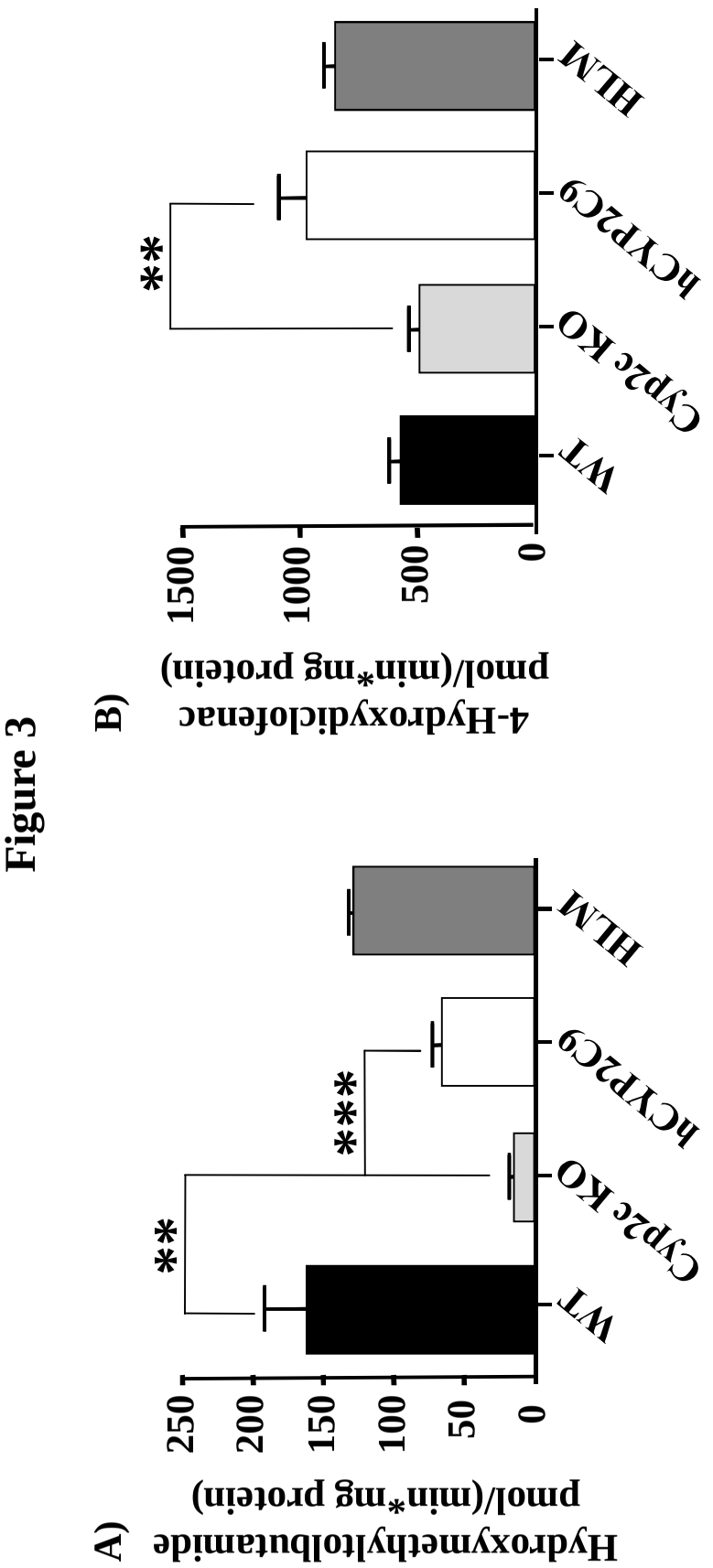

Figure 3

Figure 4

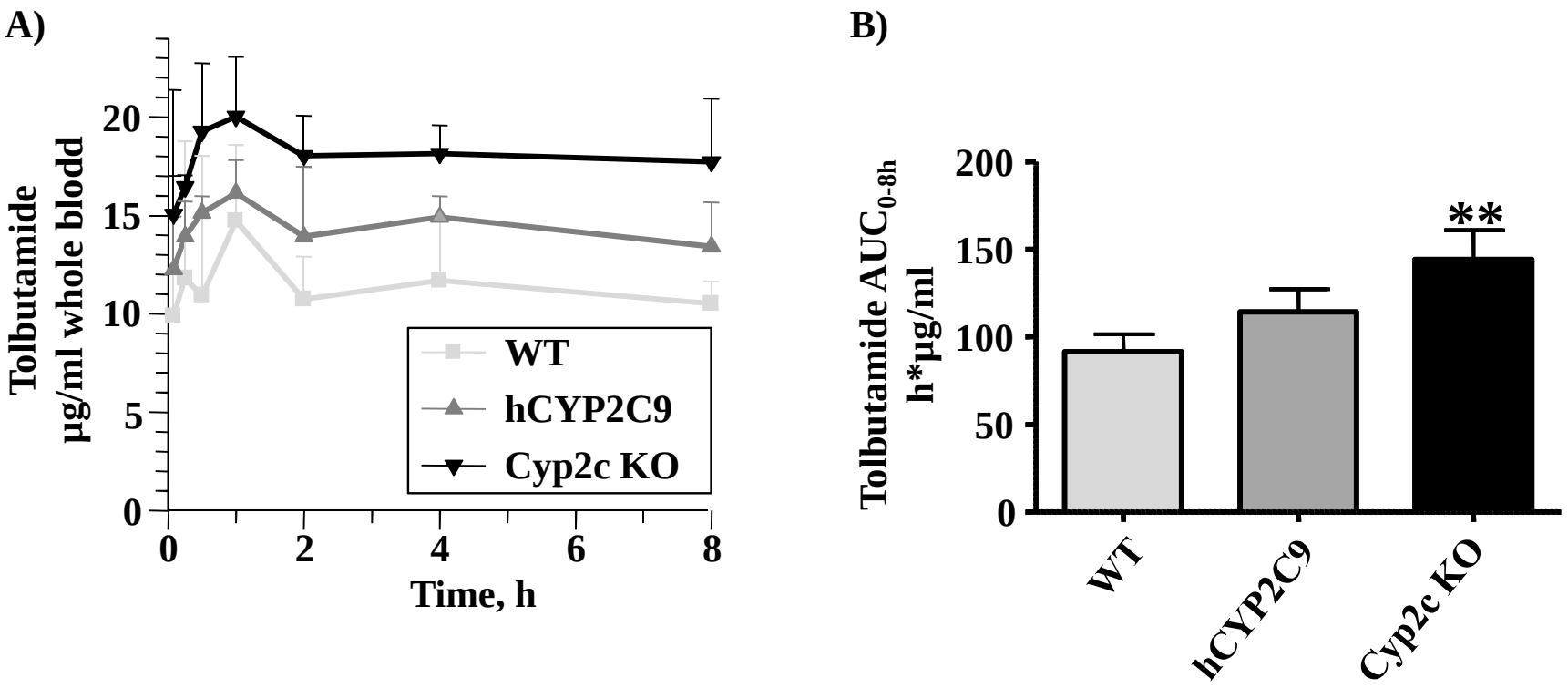

Figure 5

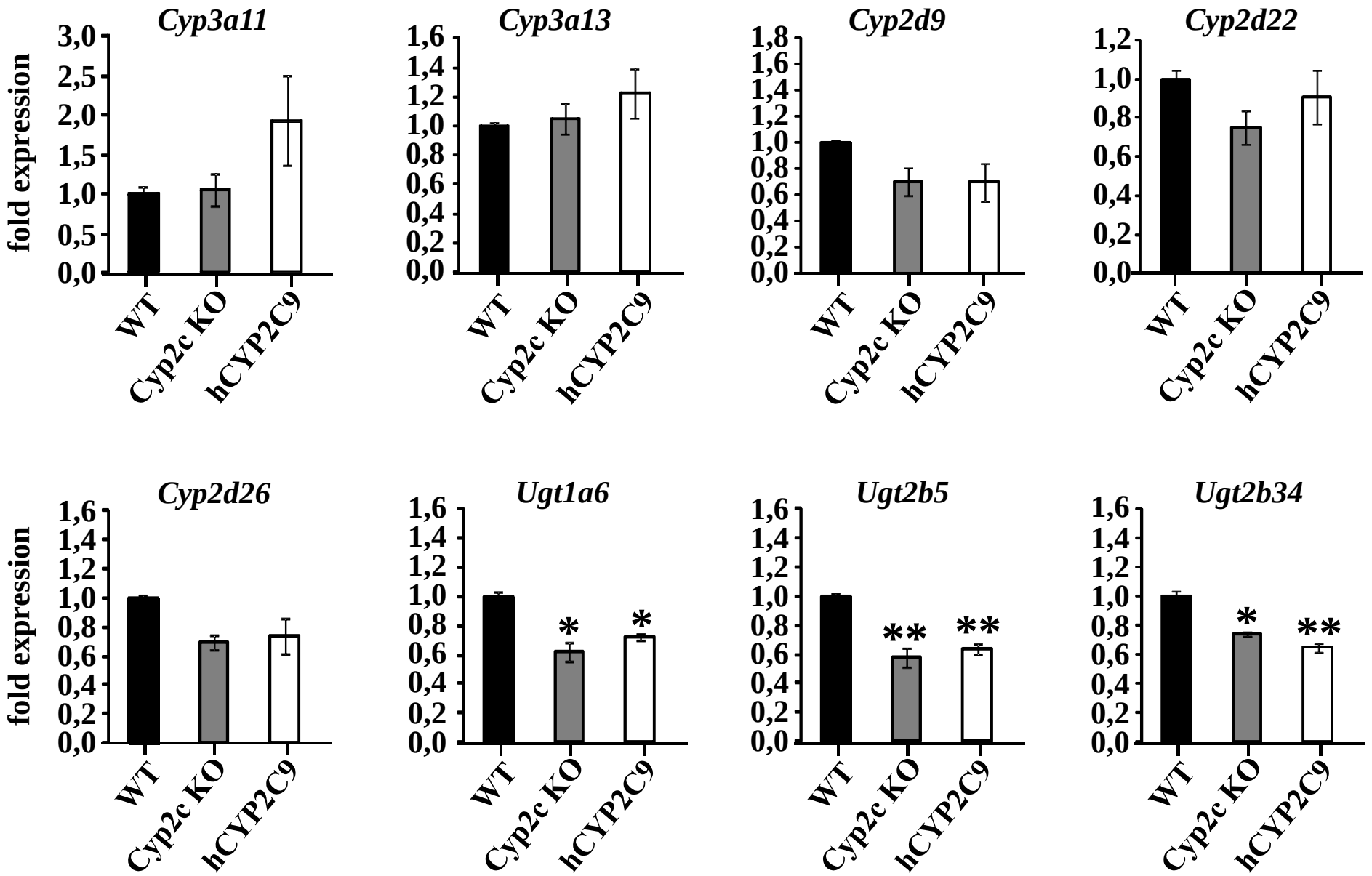

Figure 6

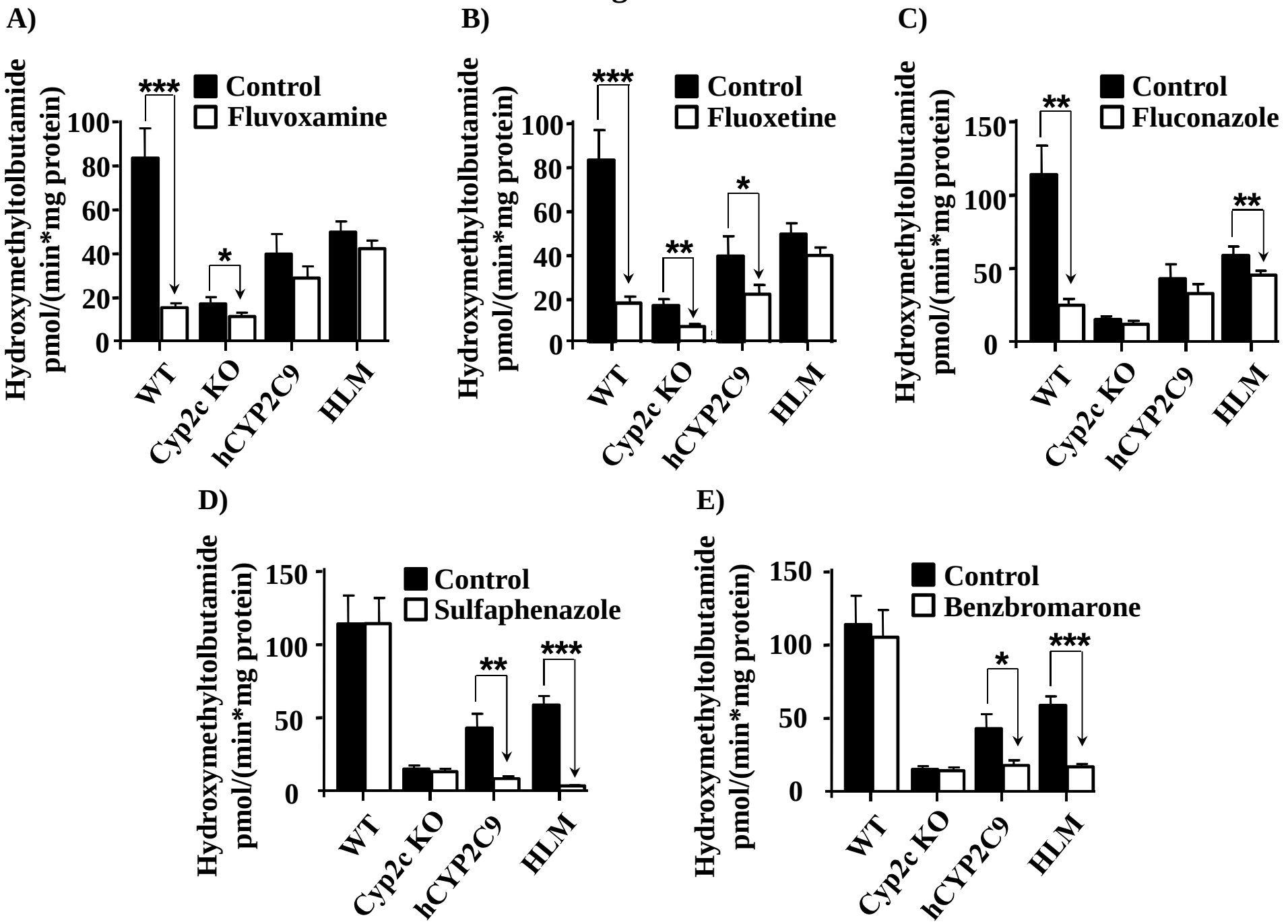

Supplementary Figure 1

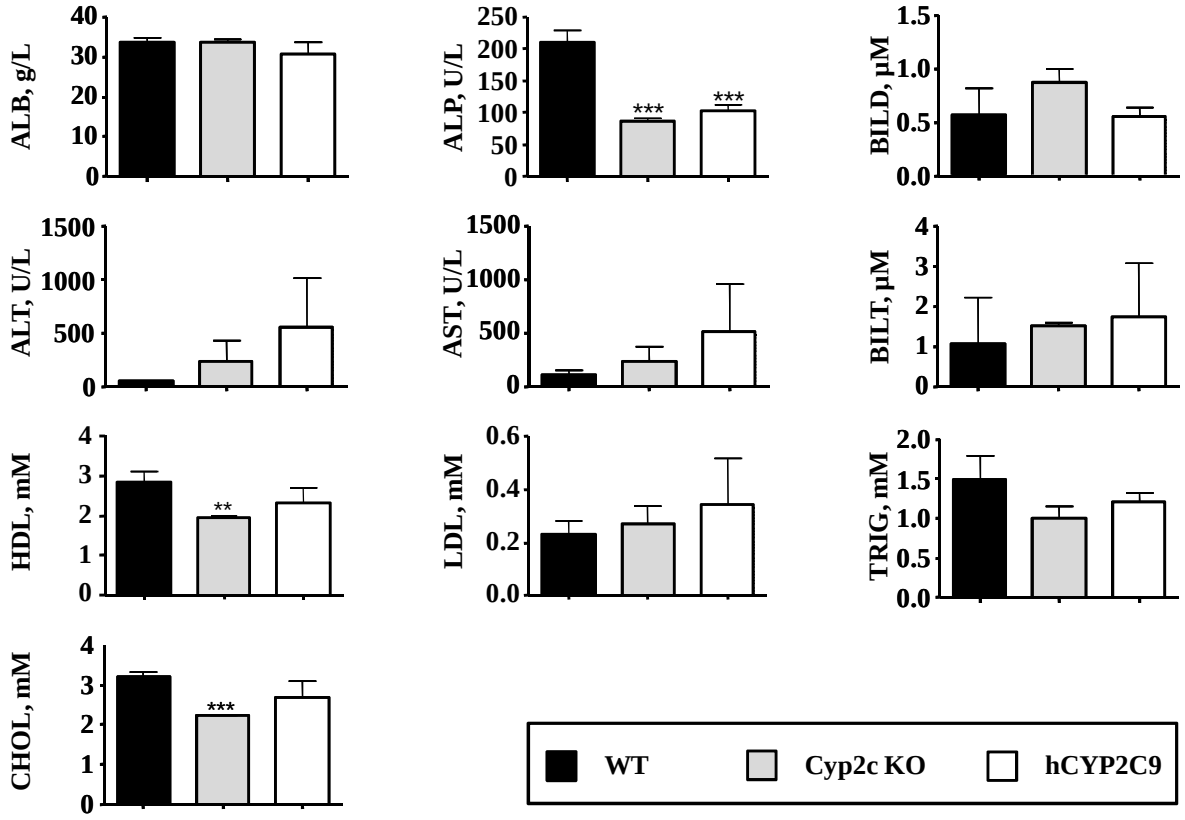

Supplementary Fig. 1: Clinical chemistry analysis of plasma from WT, Cyp2c KO and hCYP2C9 mice. Albumin (ALB), alkaline phosphatase (ALP), direct bilirubin (BILD), alanine aminotransferase (ALT), aspartate aminotransferase (AST), total bilirubin (BILT), high density lipoproteins (HDL), low density lipoproteins (LDL), triglycerides (TRIG) and cholesterol (CHOL) levels were compared between all three mouse lines (n=3 mice per line). Data are shown as mean ± SD. Transgenic mice were compared with WT animals using a Student's t-test (2-sided), with ** and *** statistically different from control at <0.01 and <0.001, respectively.

Supplementary Figure 2

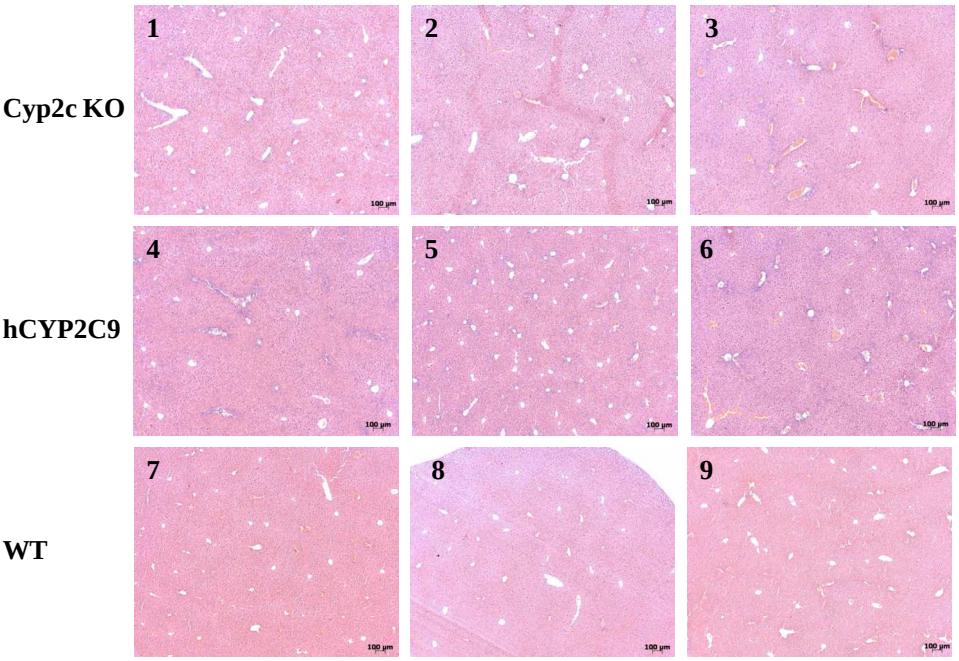

Supplementary Fig. 2: Haematoxylin and eosin analysis on liver sections from Cyp2c KO, hCYP2C9 and WT mice. Representative sections from three different mice are shown for each mouse line.

Supplementary Materials and Methods

Generation and molecular characterization of ES cell clones targeted at the Cyp2c55 and Cyp2c70 gene loci. *Cyp2c55*: The targeting vector was linearized with *Not*I and electroporated into a C57BL/6 mouse ES cell line. Of 384 G418 resistant ES cell colonies screened by standard Southern blot analyses, six correctly targeted clones were identified, expanded and further analysed by Southern blot analyses with 5' and 3' external probes and an internal neomycin probe. Five of the six clones were confirmed as correctly targeted at both homology arms. None of the five clones carried additional random integrations (data not shown). *Cyp2c70*: The targeting vector was linearized using *Not*I and electroporated into the correctly targeted *Cyp2c55* ES clone described above. Of 684 hygromycin resistant ES cell colonies screened by standard Southern blot analyses six correctly targeted clones were identified, expanded and further analysed by Southern blot analyses as described above. Five of these six clones were confirmed as correctly targeted at both homology arms without additional random integrations (data not shown).

Targeting of *Cyp2c55* and *Cyp2c70* has to be on the same allele in order to allow Cre-mediated deletion of the mouse *Cyp2c* Cluster. Therefore, four of the correctly double targeted ES cell clones described above were further analysed by in vitro deletion with Cre, followed by Gancyclovir selection and PCR analysis to detect deletion of the *Cyp2c* cluster. For *Cre*-mediated deletion of the *Cyp2c* Cluster in the double targeted ES cells, 1×10^7 ES cells derived from each of the finally validated clones were electroporated with the Cre-expression plasmid pCAGGScrepA as described previously (Seibler et al., 2005) and plated on 10 cm dishes. The Cre-transfected ES cells were grown in the presence of Gancyclovir, which is toxic in the presence of thymidine kinase (TK). Because Cre-mediated deletion of the mouse *Cyp2c* cluster will also lead to a loss of the TK selection cassette (Fig. 1E), only ES

cell clones with targeting of *Cyp2c55* and *Cyp2c70* on the same allele survived the Gancyclovir selection. Approximately 200-300 cells survived this selection in two of the four clones tested. Gancyclovir resistant cells from one of the two clones (A-C10) was transferred to individual wells of a 96-well plate, expanded and further analysed by PCR and Southern Blot analysis, confirming the successful deletion of the *Cyp2c* cluster in these cells (data not shown). *Cyp2c* deleted ES cell clones were used to generate Cyp2c KO mice and were further modified by the insertion of a CYP2C9 expression cassette (see below).

In order to generate ES cell clones with a replacement of the mouse *Cyp2c* cluster with a CYP2C9 expression cassette, a targeting vector was generated in which a cDNA of *CYP2C9* containing the original human *CYP2C9* intron 4 was linked to a fusion of the 8.5-10.4 kb BamHI/NheI enhancer and 0.3 kb promoter fragment of the mouse albumin upstream regulatory region (Pinkert et al., 1987). This targeting vector also contained *loxP*, *lox5171* and *f3* sites, polyadenylation and splice acceptor polyadenylation motifs and a 5' deficient neomycin selection cassette as depicted in Fig. 1F. This allowed the insertion of the CYP2C9 expression cassette via Cre-mediated recombination at the corresponding *lox* sites in the prepared *Cyp2c* deleted ES cell clones (see above) and selection of correctly targeted clones with high stringency by the complementation of the deficient neomycin cassette with the promoter and ATG remaining at the deleted *Cyp2c* locus (Fig. 1G). For this purpose, $1x10^7$ cells were electroporated under standard conditions with supercoiled targeting vector and the Cre-expression plasmid pCAGGScrepA as previously described (Seibler et al., 2005) and selected with G418. 11 G418 resistant ES cell clones were obtained after the electroporation procedure. Six of the clones were expanded and further analysed by PCR and Southern blot with different suitable restriction enzymes, 5′ and 3′ external probes, and an internal neomycin probe. Five of the six clones were confirmed as correctly recombined at both *lox* sites, were shown to carry a single copy of the integrated CYP2C9 expression cassette

and didn't carry additional random integrations. One of these clones was used to generate the hCYP2C9 mice. The neomycin selection cassette was subsequently deleted in vivo by flipase recombinase (Flp) mediated recombination at the *f3* recognition sites (Fig. 1H).

Molecular characterization of CYP2C9 humanized and Cyp2c KO mice. Offspring from chimeras derived from *Cyp2* cluster deleted ES cells or ES cells with an insertion of the CYP2C9 expression cassette were analysed by PCR in order to determine the genotype of these mice. The following PCR primer pairs were used for the detection of the different alleles: (1) WT mouse *Cyp2c* cluster allele: 5'-CTACAATGCTCTGCCTACCC-3' and 5'-AAATCTGACTCCCTCTTCTGG-3', resulting in a 307 bp PCR fragment; (2) Deleted *Cyp2c* cluster allele: 5'-GACATTGACATCCACTTTGCC-3' and 5'-GATGGATGTGTGGAATGAAGAG-3', resulting in a 559 bp PCR fragment and (3) Allele with CYP2C9 expression cassette: 5'-GCAGGCCAGAGTCCATTCAG-3' and 5'-CTGGAGTGGCAACTTCCAG-3', resulting in a 712 bp PCR fragment. Mice heterozygous for the deletion of the mouse *Cyp2c* cluster or carrying the CYP2C9 expression cassette were crossed to generate homozygous Cyp2c KO and hCYP2C9 mice, respectively. Homozygosity was determined by the presence of the corresponding modified allele and absence of the 307 bp WT PCR fragment.

Preparation of tissues. Terminal blood samples were mixed on a roller for 5 minutes at room temperature. Erythrocytes were removed by centrifugation (2,000 – 3,000 rpm for 10 min at 8 - 10°C) and the resulting plasma was stored on ice prior to clinical chemistry analysis. The gall bladder was removed and the liver removed and weighed. Two samples of liver (30 mg +/- 10%) were cut into smaller pieces and placed into two separate cryovials prior to addition of RNAlater (1.8 ml). Samples were incubated at +4^{o}C overnight and then stored at approximately -70^{o}C before TaqMan analysis. The remaining liver was weighed and used

immediately for subcellular fractionation by differential centrifugation according to standard methods. Mouse liver microsomes were prepared and stored as described recently (Scheer et al., 2008).

Immunoblot analysis of Cyp2c and CYP2C9 protein expression. The expression of Cyp2c and CYP2C9 apoproteins was visualized in liver microsome samples by immunoblot analysis. A human CYP2C9/19-specific antibody (a rabbit polyclonal anti-CYP2C9/19 developed in house by CXR Biosciences) was used to detect the human CYP2C9 and a polyclonal rabbit anti-Cyp2c1 antibody (kindly provided by Dr. Colin Henderson, University of Dundee, UK) was used to detect mouse Cyp2c apoproteins. 10 μg of microsomal protein were loaded for the immunoblots. The positive controls were pooled human liver microsomes (BD Biosciences, #452161), and recombinant human CYP2C9 (0.1 pmol) (Lifetechnologies, #P2378, Grand Island, NY).

Quantitative Reverse Transcriptase-PCR (qRT-PCR). qRT-PCR and analysis was carried out as described previously (Hasegawa et al., 2011). Primers used were from the following Assay-On-Demand Kits (Applied Biosystems, Foster City, CA): Hs00426397_m1 (*CYP2C9*), Mm00656110_gH (*Cyp2c39*), Mm01197188_m1 (*Cyp2c44*), Mm00472168_m1 (*Cyp2c55*), Mm00521058_m1 (*Cyp2c70*), Mm00731567_m1 (*Cyp3a11*), Mm00484110_m1 (*Cyp3a13*), Mm00651731_m1 (*Cyp2d9*), Mm00530542_m1 (*Cyp2d22*), Mm01307122_g1 (*Cyp2d26*), Mm01967851_s1 (*Ugt1a6*), Mm01623253_s1 (*Ugt2b5*) and Mm00655373_m1 (*Ugt2b34*).

In vitro determination of CYP2C-dependent activities. A tolbutamide (100 μM) microsome (0.5 mg protein/ml) mixture in phosphate buffer (100 mM KH_2PO4 pH7.4, 3.3 mM $MgCl_2$) was incubated in a water bath for 5 min at 37^{o}C prior to the start of the reaction by addition of NADPH regenerating system (final concentrations: 1.3 mM NADPH, 4 mM glucose-6-phosphate, 2 U/ml glucose-6-phosphate dehydrogenase). After 30 min, the reaction

was stopped by addition of an equal volume of ice-cold acetonitrile containing dextrorphan (1 μM) as internal standard. Samples were centrifuged for approximately 15 minutes at approximately 3,500 g on a Legend RT centrifuge (Sorvall, Newton, CT) and concentration of hydroxymethyltolbutamide in the supernatant determined by LC-MS/MS. Calibration standards were prepared in the phosphate buffer/acetonitrile with the internal standard (1:1 v/v; centrifuged (10 min, ~16000g) on a Biofuge Fresco centrifuge (Sorvall, Newton, CT)) by adding an appropriate amount of hydroxymethyltolbutamide. Chromatographic separation was performed on a Luna, C18 column (5μm, 150 x 2.0mm) (Phenomenex, Macclesfield, UK) using an injection volume of 10 μl and a run time of 4.51 minutes. The detector used was a Micromass Quattro Micro mass spectrometer (Micromass UK Ltd, Manchester, UK) run in electrospray positive ion mode. The multiple reaction monitoring parameters for hydroxymethyltolbutamide and dextrorphan were 287.31 and 258.2 (parent ions) and 171.25 and 199.3 (collision ions), respectively.

A diclofenac (4 μM) microsome (0.25 mg protein/ml) mixture in phosphate buffer (100 mM KH_2PO4 pH7.4, 3.3 mM $MgCl_2$) was incubated in a water bath for 5 min at 37^{o}C prior to the start of the reaction by addition of NADPH (1 mM final concentration). After 5 min, the reaction was stopped by addition of an equal volume of ice-cold acetonitrile containing dextrorphan (1 μM) as internal standard. Samples were centrifuged for approximately 15 minutes at approximately 3,500 g on a Legend RT centrifuge (Sorvall, Newton, CT) and 4-hydroxydiclofenac concentrations in the supernatant were determined by LC-MS/MS. Calibration standards were prepared in the phosphate buffer/acetonitrile with the internal standard (1:1 v/v; centrifuged (10 min, ~16000g) on a Biofuge Fresco centrifuge (Sorvall, Newton, CT)) by adding an appropriate amount of 4-hydroxydiclofenac. Chromatographic separation was performed on a Luna, C18 column (5μm, 150 x 2.0mm) (Phenomenex, Macclesfield, UK) using an injection volume of 10 μl and a run time of 4.51 minutes. The

detector used was a Micromass Quattro Micro mass spectrometer (Micromass UK Ltd, Manchester, UK) run in electrospray positive ion mode. The multiple reaction monitoring parameters for 4-hydroxydiclofenac and dextrorphan were 312.04 and 258.2 (parent ions) and 230.06 and 199.3 (collision ions), respectively.

Pharmacokinetic analysis for tolbutamide. Tolbutamide solution in ethanol (5 mg/ml) was diluted 10 times by PEG200 solution in PBS (2:1; v/v) and administered intraperitoneally (5 mg/kg body weight) to all animals. The volume of dosing solution was 10 ml/kg bodyweight. For the analysis of tolbutamide pharmacokinetics, blood (10 µl aliquots) samples were collected at 0.083, 0.25, 0.5, 1h, 2h, 4h, 8h after dosing, placed immediately into microfuge tubes containing 10 µl MilliQ water, snap frozen in liquid nitrogen and stored at approximately -70ºC prior to analysis. Concentrations of tolbutamide in whole blood were measured by LC/MS/MS. Calibration standards were prepared in whole blood water (1:1 v/v; 95 µl) by adding an appropriate amount of tolbutamide in acetonitrile (5 µl). 20 µl of the test samples and of the calibration standards were extracted in 80µL of acetonitrile containing 500ng/ml dextrorphan as an internal standard. The mixture was vortexed for approximately 30 sec, sonicated in an ultrasonic water-bath for 30 sec and centrifuged at approximately 13,000 g for 5 minutes. The supernatant was transferred to a 96-well plate and the concentrations tolbutamide and dextrorphan were measured by LC/MS/MS. Chromatographic separation was performed on a Luna, C18(2) column (5µm, 150 x 2 mm) (Phenomenex, Macclesfield, UK) using an injection volume of 10 µl and a run time of 5.5 minutes. The detector used was a Micromass Quattro Micro mass spectrometer (Micromass UK Ltd, Manchester, UK) run in electrospray positive ion mode. The multiple reaction monitoring parameters for tolbutamide and dextrorphan were 271.15 and 258.2 (parent ions) and 73.64 and 199.2 (collision ions), respectively. Pharmacokinetic parameters were calculated using WinNonlin Professional version 5.2 (Pharsight, Mountain View, CA).

In vitro CYP2C inhibition studies. A tolbutamide (100 µM) microsome (0.5 mg protein/ml) mixture in phosphate buffer (100 mM KH_2PO4 pH7.4, 3.3 mM $MgCl_2$) was incubated with and without an inhibitor (final inhibitor concentrations: 2 µM fluvoxamine; 15 µM fluoxetine; 5 µM fluconazole; 50 µM sulfaphenazole and 0.25 µMbenzbromarone) in a water bath for 5 min at 37^{o}C prior to the start of the reaction by addition of NADPH regenerating system (final concentrations: 1 mM NADPH, 4 mM glucose-6-phosphate and 2 Units/ml glucose-6-phosphate dehydrogenase). After 20 min, the reaction was stopped by addition of an equal volume of ice-cold acetonitrile containing bupropion (10 ng/ml) as an internal standard. Samples were centrifuged for approximately 15 minutes at approximately 3,500 g on a Legend RT centrifuge (Sorvall,Newton, CT) and hydroxymethyltolbutamide concentrations in the supernatant were determined by LC-MS/MS. Calibration standards were prepared in the phosphate buffer/acetonitrile with the internal standard (1:1 v/v; centrifuged (10 min, ~16000g) on a Biofuge Fresco centrifuge (Sorvall, Newton, CT)) by adding an appropriate amount of hydroxymethyltolbutamide. Chromatographic separation was performed on a Luna, C18(2) column (5µm, 150 x 2.0mm) (Phenomenex, Macclesfield, UK) using an injection volume of 10 µl and a run time of 4.51 minutes. The detector used was a Micromass Quattro Micro mass spectrometer (Micromass UK Ltd, Manchester, UK) run in electrospray positive ion mode. The multiple reaction monitoring parameters for hydroxymethyltolbutamide and bupropion were 287.33 and 240.31 (parent ions) and 171.11 and 184.17 (collision ions), respectively.

Supplementary Methods References

Hasegawa M, Kapelyukh Y, Tahara H, Seibler J, Rode A, Krueger S, Lee DN, Wolf CR and Scheer N (2011) Quantitative prediction of human pregnane X receptor and cytochrome P450 3A4 mediated drug-drug interaction in a novel multiple humanized mouse line. *Mol Pharmacol* **80**(3):518-528.

Pinkert CA, Ornitz DM, Brinster RL and Palmiter RD (1987) An albumin enhancer located 10 kb upstream functions along with its promoter to direct efficient, liver-specific expression in transgenic mice. *Genes Dev* **1**(3):268-276.

Scheer N, Ross J, Rode A, Zevnik B, Niehaves S, Faust N and Wolf CR (2008) A novel panel of mouse models to evaluate the role of human pregnane X receptor and constitutive androstane receptor in drug response. *J Clin Invest* **118**(9):3228-3239.

Seibler J, Kuter-Luks B, Kern H, Streu S, Plum L, Mauer J, Kuhn R, Bruning JC and Schwenk F (2005) Single copy shRNA configuration for ubiquitous gene knockdown in mice. *Nucleic Acids Res* **33**(7):e67.